Microsc. Microanal. Microstruct. **4** (1993) 323–330 APRIL/JUNE **1993**, PAGE 323

Classification
Physics Abstracts
07.80 — 61.80J

In-situ observation of damage evolution in aluminium irradiated with H and He ions

S. Furuno([1]), K. Hojou([1]), H. Otsu([1]), K. Izui([2]), N. Kamigaki([3]), K. Ono([4]) and T. Kino([5])

([1]) Department of Materials and Engineering, Japan Atomic Energy Research Institute, Tokai-mura, Ibaraki 319-11, Japan
([2]) Faculty of Education, Nagasaki University, Nagasaki 852, Japan
([3]) Faculty of Education, Ehime University, Matsuyama 790, Japan
([4]) Faculty of Science, Shimane University, Matsue 690, Japan
([5]) Hiroshima Denki Institute of Technology, Aki-ku, Hiroshima 739-03, Japan

(Received March 1, 1993 ; accepted June 15, 1993)

Abstract. — The behavior of bubbles and blisters in aluminum during 10 keV He^+ ion irradiation at 573 K was investigated. Processes of the evolution of surface damage were clarified using an *in-situ* electron microscope observation system. The difference among irradiation effects obtained by three kinds of experiments at room temperature was examined using both 15 keV H_2^+ and 12 keV He^+ ions. The obtained results were interpreted by difference in the production rate of vacancies introduced by gas implantation and different mobility of these two ions in aluminum.

1. Introduction.

In order to simulate the structural and chemical changes due to plasma-wall interaction in fusion reactor materials, ion irradiation experiments have been performed. For these activities, *in-situ* observation on dynamic process of damage evolution is a useful technique to establish a reliable physical model [1, 2]. We developed an *in-situ* observation system consisting of a 100 kV electron microscope linked with a 10 kV ion accelerator in 1986 [3].

We observed dynamic behavior of helium bubbles in aluminum during 10 keV He^+ ion irradiation at various temperatures and following annealing using this equipment [4].

The dynamic growth behavior of hydrogen bubble in aluminum during 10 keV H_2^+ ion irradiation and the shrinkage of the bubbles during following annealing were also observed. The binding energy between vacancy and bubble was estimated to be about 0.4 eV from the shrinkage behavior of the bubbles [5].

For the radiation damage of fusion reactor materials, dual-ion beam irradiation is more desirable, because various ions are simultaneously impinging to the surface of the wall from the plasma gas.

In order to clarify the main factors influencing on bubble formation and its growth, we performed dual-ion beam irradiation experiments using an 400 kV electron microscope combined with two sets of 40 kV ion accelerators [6]. It was found that vacancy production rate and gas injection rate were important factors to determine the bubble nucleation, its number density and size [7].

This paper reports the results of *in-situ* observation of bubbles in aluminum during 10 keV He^+ single ion irradiation at 573 K and the difference in irradiation effects obtained by three kinds of experiments at room temperature: 1) irradiating 15 keV H_2^+ ions and 12 keV He^+ ions simultaneously, 2) irradiating 15 keV H_2^+ ions after 12 keV He^+ ion pre-irradiation and 3) irradiating 12 keV He^+ ions after 15 keV H_2^+ ion pre-irradiation.

2. Experimental procedure.

2.1 *In-situ* observation systems. — The *in-situ* observation system during single ion irradiation consists of JEM-100 C type electron microscope and a Duo-plasmatron type ion gun with accelarating voltage of 10 kV, as shown in figure 1. The ion beam is mass-selected through a magnet and then introduced in the horizontal direction into the specimen chamber of the electron microscope. Inside the specimen chamber the beam is deflected downward by an angle of 72° with the electrostatic prism so as to be incident on the specimen surface at this angle, as shown in figure 2.

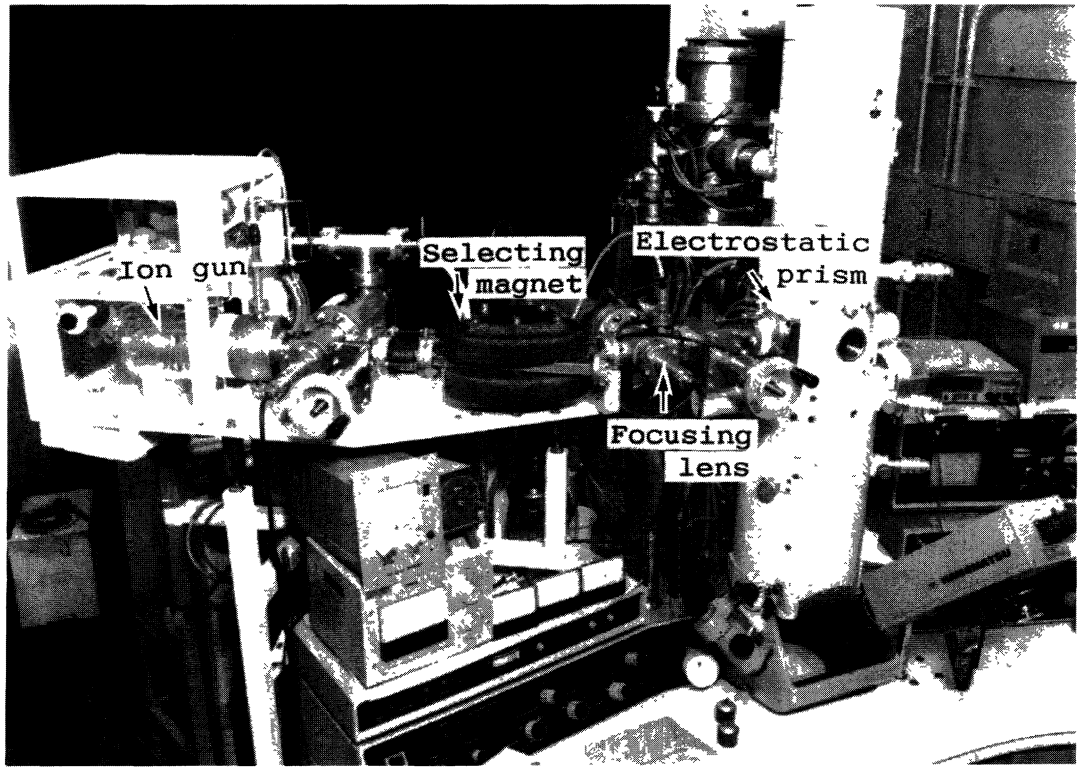

Fig. 1. — Overall view of the equipment for *in-situ* observation during single ion irradiation.

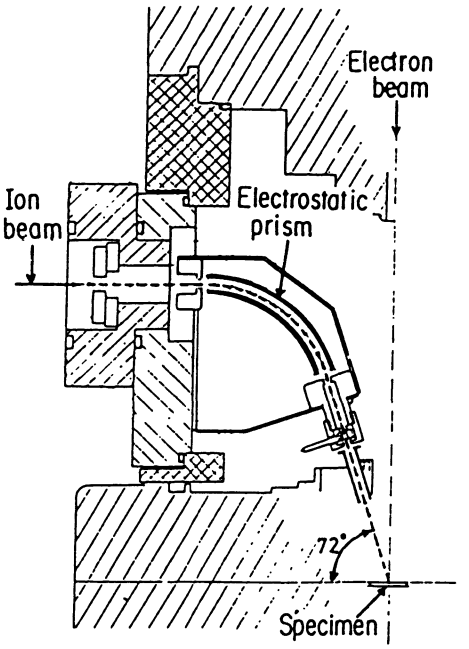

Fig. 2. — Schematic diagram of electrostatic prism set in the chamber of electron microscope.

The *In-situ* observation system during dual-ion irradiation consists of JEM-4000 FX type electron microscope linked with two sets of 40 kV ion accelerators. The angle of the mass-selected ion beam is 60° to the specimen surface, as shown in figure 3.

Results of *in-situ* observation during ion irradiations were recorded using VTR through TV camera and TV monitor.

2.2 Specimens. — Used specimens were zone-refined aluminum of 99.9999% purity [8]. Thin films for electron microscope observation were made by electropolishing in a mixed solution of ethanol and perchloric acid in the ratio of 4:1.

2.3 Single ion irradiation. — The irradiation was carried out at 10 keV He^+ ions with the flux of 3×10^{17} ions/m^2s at 573 K.

2.4 Dual-ion irradiation. — 15 keV H_2^+ and 12 keV He^+ ions were used for dual-ion irradiation. All of these ions almost stop within the aluminum foil of about 20 nm in thickness, which was calculated from the TRIM-code [7]. The irradiations were performed at room temperature. The elctron microscope was operated at 150 kV to avoid damage due to electron irradiation. The irradiation conditions were as follows.

1) Simultaneous He^+ and H_2^+ dual-ion irradiation for 40 minutes. The fluxes of He^+ ions and H_2^+ were 2.5×10^{17} ions/m^2s and 1.25×10^{17} ions/m^2s, respectively, and these corresponded to the atomic fluxes of 2.5×10^{17} atoms/m^2s.

2) H_2^+ ion irradiation for 20 minutes after He^+ ion pre-irradiation for 20 minutes. The atomic fluxes of each ion were 5×10^{17} atoms/m^2s.

3) He^+ ion irradiation for 20 minutes after H_2^+ ion pre-irradiation for 20 minutes. The atomic

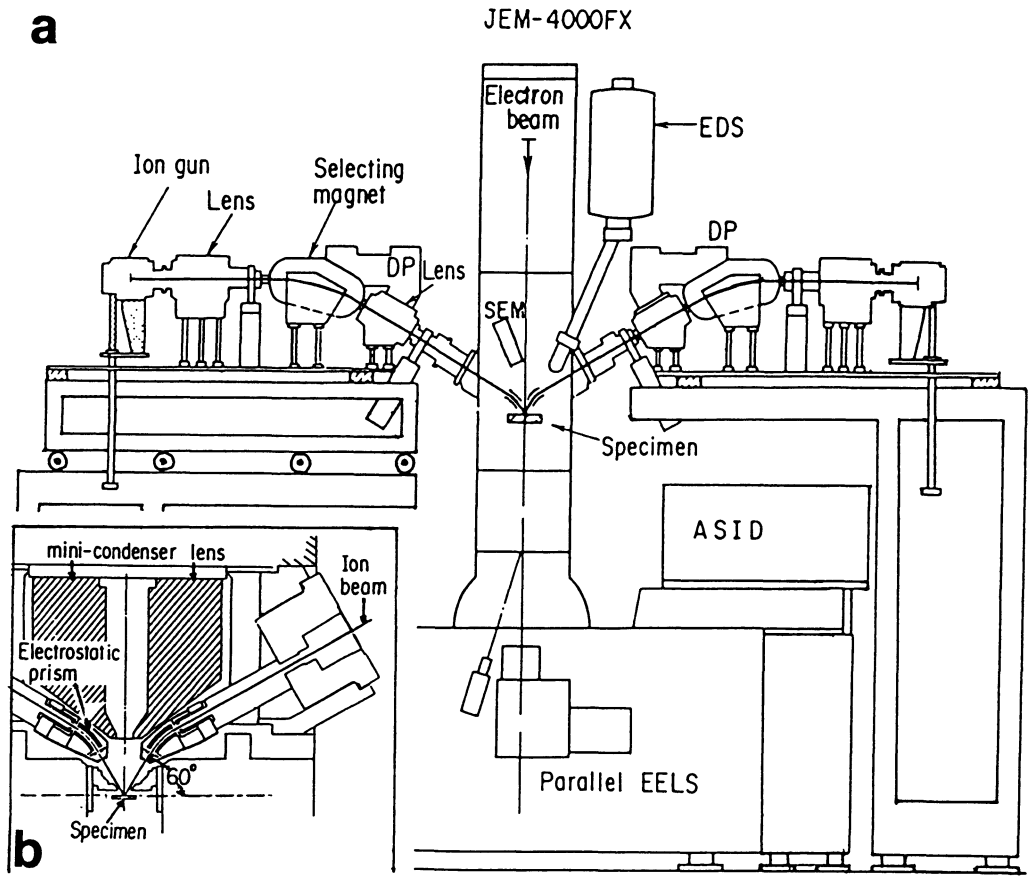

Fig. 3a. — Schematic diagram of the system for *in-situ* observation during dual-ion irradiation. b) Closed up schematic diagram of electrostatic prism in the chamber of electron microscope.

fluxes of each ion were 5×10^{17} atoms/m^{2}s.

3. Experimental results and discussion.

3.1 Single ion irradiation with He^+ ions. — Dynamic behaviors of bubbles in aluminum were clarified by *in-situ* observation during irradiation with 10 keV He^+ ions. Typical example was shown in figures 4 for irradiation at 573 K with the flux of 3×10^{17} ions/m^{2}s.

Bubbles were formed within 10 minutes and increased gradually in its number and size. Figures 4a to d show the initial stage of bubble growth. Some bubbles grew due to rapid coalescence. Sudden burst and exfoliation of bubbles occured within about 3 hours as shown in figures 4d to e. The underlying bubbles grew again. This process was repeated. During these processes, hole are often formed in the region where large bubbles burst. These holes increased in its number and size, as the irradiation proceeded. Some holes shrank gradually and disappeared, as indicated with arrows in figures 4e to h. In the periphery of expanding hole, some bubbles were observed as blisters on the surface of the specimen, as indicated with arrows in figure 4i to k. These blisters burst, as hole expansion proceeded.

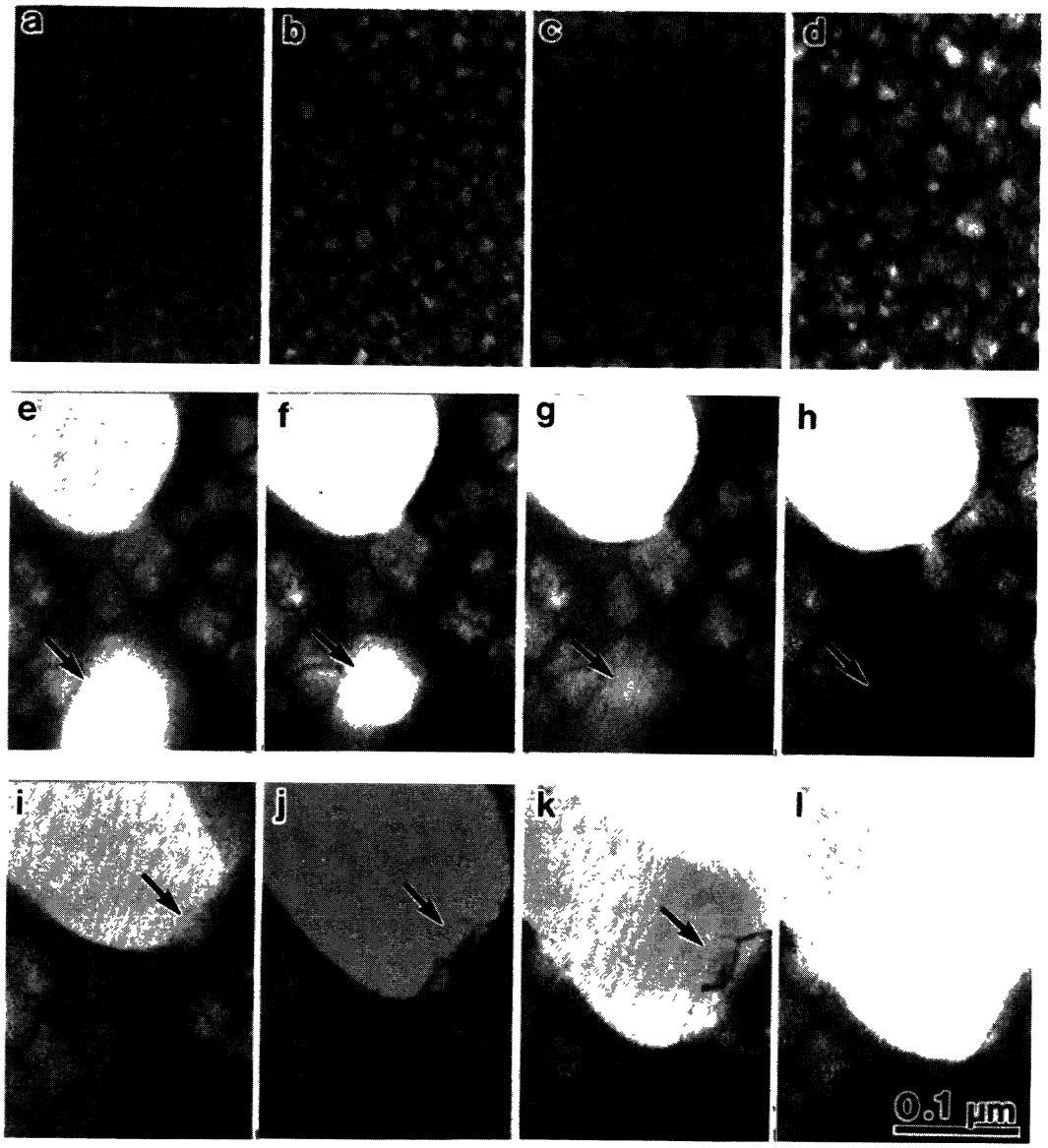

Fig. 4. — Dynamic behavior of bubbles and blisters during 10 keV He^+ ion irradiation at 573 K with the flux of 3×10^{17} ions/m^2s. Irradiation time: a) 47 minutes, b) 1 hour 6 minutes, c) 2h 11m, d) 3 h, e) 3h 4m 13s, f) 3h 4m 22s, g) 3h 4m 25s, h) 3h 4m 29s, i) 3h 4m 29s, j) 3h 4m 31s, k) 3h 4m 33s, and l) 3h 4m 34s.

Bubbles were formed throughout the specimen, and then seemed to move gradually toward the surface with bubble growth. When bubbles grew up near the surface, then they contacted with each other, as shown in figure 4d. As the irradiation proceeds, implanted helium would be

accumulated in the bubble and may raise the inner pressure of bubble. At this moment, if the bubble has a weak place irresistible to the inner pressure, a burst may occur, helium gas in the bublle would pour out from the surface and bubbles on the surface disappear, as seen in figures 4d to e. Expansion and shrinkage of holes as shown in figures 4 (e-l) suggest that aluminum atoms in large amount can easily move at 573 K. By repeating these dynamic processes, the surface undergoes erosion successively as the irradiation proceeds.

3.2 Dual-ion irradiation and following ion irradiation with He^+ and H_2^+ ions. — Figure 5 (1) shows the results of H_2^+ and He^+ dual-ion irradiation. Bubbles were formed within 5 minutes and then grew gradually. Figure 5 (2) shows the results of H_2^+ ion irradiation after He^+ ion pre-irradiation. During pre-irradiation (Fig. 5 (2) (a) and (b)), bubbles grew slowly, but during H_2^+ ion irradiation, bubbles grew large as indicated with arrows in figure 5 (2) (d). Figure 5 (3) shows the results of He^+ ion irradiation after H_2^+ ion pre-irradiation. During pre-irradiation (Figs. 5 (3) (a and b)) bubbles grew large, but its number density is extremely low. During following He^+ ion irradiation (Figs. 5 (3) (c and d)), bubbles grew slowly with increasing number density. Large bubbles were observed to grow on hydrogen bubbles formed during pre-irradiation as indicated with arrows in figure 5 (3) (d).

The difference among the observed results is considered to be mainly due to a difference in the production rate of point defects produced by 15 keV H_2^+ and 12 keV He^+ ion irradiations and the different mobility of hydrogen and helium atoms injected by irradiations in aluminum. The ratio of the production rate due to 12 keV He^+ ion and 7.5 keV H^+ ion was estimated to be about 10: 1 from the results of TRIM-code calculations [7].

In the case of He^+ ion irradiation, the number of vacancies which acts as trapping sites for helium atoms is large, as shown in figures 5 (2) (a-b). If the gas atoms trapped in vacancies migrate by vacancy mechanism and encounter with each other to form di-gas atoms trapped in vacancies, they act as stable nuclei for bubbles. The number of nuclei for bubbles becomes large. The amount of gas atoms supplied for each nuclei in the process of ion irradiation decreases. Consequently helium bubbles increase in number density and decrease in size.

On the other hand, in the case of H_2^+ ion irradiation, as shown in figures 5 (3) (a-b), a large fraction of hydrogen atoms will escape away from the surface, because the number of irradiation-induced vacancies is very small. Furthermore, the implanted hydrogen atoms are highly mobile, even if they are trapped in vacancies [5, 9]. As the surface of thin specimen acts as strong sink for hydrogen atoms, the number of hydrogen atoms will decrease. Accordingly the production of di-hydrogen atoms trapped in vacancies is lower. In spite of low concentration of hydrogen atoms, the amount of hydrogen atoms supplied for each bubble will increase, because of high mobility of hydrogen atoms and low concentration of bubbles. Consequently hydrogen bubbles with very small number density can grow large.

During H_2^+ ion irradiation after He^+ ion irradiation, as shown in figure 5 (2) (d), the pre-formed small helium bubbles with high density act as effective trapping sites for hydrogen atoms, therefore the amount of hydrogen atoms escaping to the specimen surface is lower. Consequently the amount of hydrogen atoms supplied for bubbles become large, resulting in large growth of bubbles.

During He^+ ion irradiation after H_2^+ ion irradiation, as shown in figures 5 (3) (d), small bubbles are newly formed in large number due to large production rate of vacancies by He^+ ion irradiation. Only on some hydrogen bubbles formed by pre-irradiation, helium bubbles seem to increase in size by absorbing hydrogen atoms from hydrogen bubbles.

In the case of dual-ion irradiation, an average production rate of vacancies is larger than that in H_2 ion irradiation and less than in the He^+ ion irradiation. An average mobility of gas atoms mixed with hydrogen and helium atoms is larger than that of helium atoms and less than that

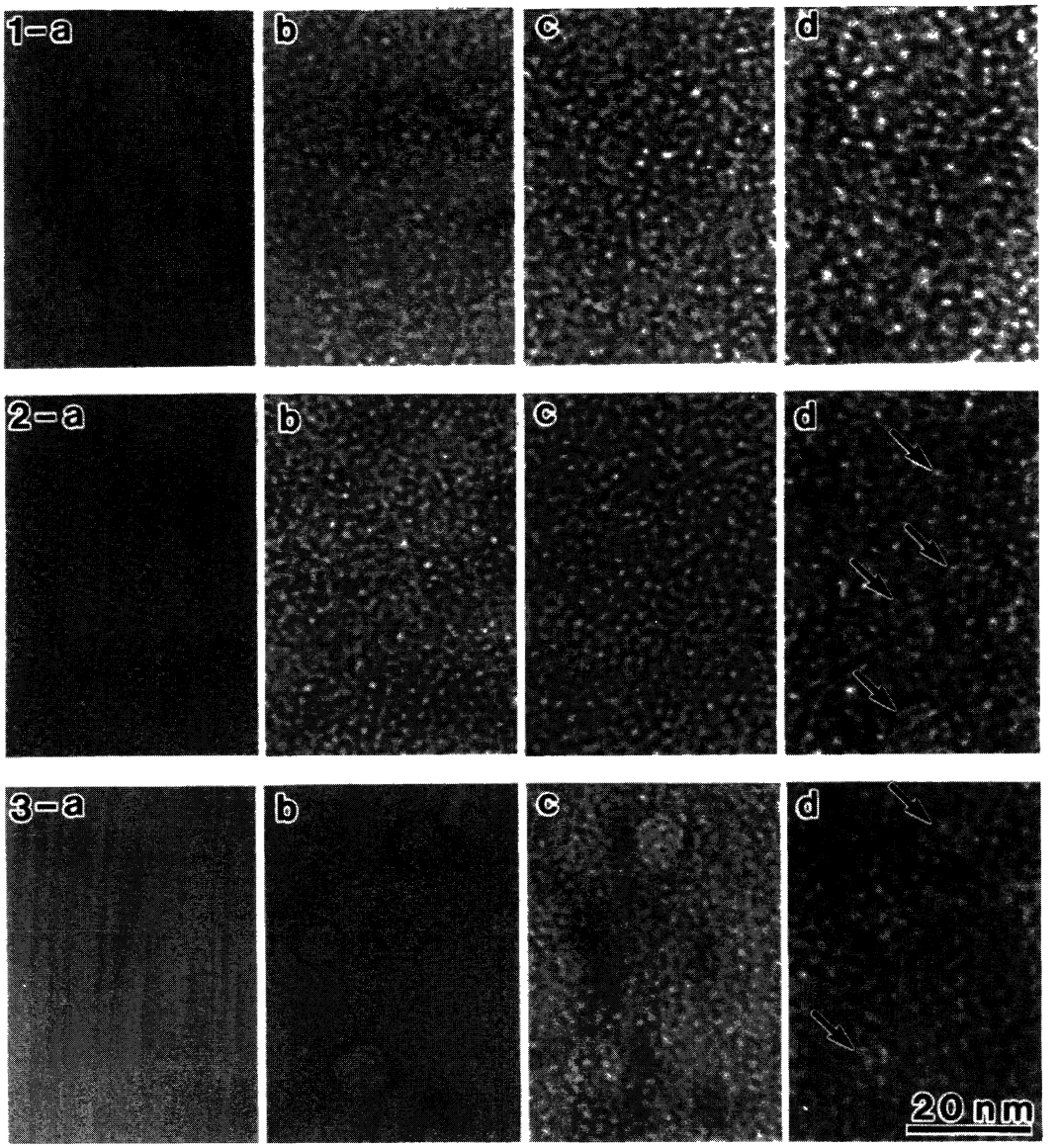

Fig. 5. — The growth of bubbles during 12 keV He^+ and 15 keV H_2^+ dual and successive ion irradiations at room temperature. Line (1): He^+ and H_2^+ dual ion irradiation with the fluxes of 2.5×10^{17} ions/m^2s and 1.25×10^{17} ions/m^2s, respectively. Line (2): He^+ ion irradiation with the flux of 5×10^{17} ions/m^2s (a) and (b), following H_2^+ ion irradiation with the flux of 2.5×10^{17} ions/m^2s (a) and (b). Line (3): H_2^+ ion irradiation with the flux of 2.5×10^{17} ions/m^2s (a) and (b), following He^+ ion irradiation with the flux of 5×10^{17} ions/m^2s. Irradiation time: Column (a) 10 minutes, column (b) 20 minutes, column (c) 30 minutes and column (d) 40 minutes, respectively.

of hydrogen atoms. Therefore, the number density of bubbles is smaller than that in He^+ ion irradiation and larger than that in H_2^+ ion irradiation, and the size of bubbles is larger than that

in He^+ ion irradiation and smaller than that in H_2^+ ion irradiation.

4. Conclusion.

In-situ observation disclosed dynamic behavior of bubbles during helium ion irradiation of aluminum.

1) Bubbles grow uniformly in the initial stage, and then suddenly burst away.

2) After this first stage of exfoliation, underlying bubbles grow to larger bubbles, which suddenly disappear again by burst. These processes occur repeatedly during irradiation, resulting in the successive erosion of the surface layer.

From the results of dual and successive ion irradiation experiments, the following conclusions were obtained:

1) Bubbles grow gradually during dual-ion irradiation.

2) In the case of H_2^+ ion irradiation after He^+ ion irradiation, small bubbles with large number density are formed during pre-irradiation, and the growth of bubbles is remarkable during following irradiation.

3) In the case of He^+ ion irradiation after H_2^+ ion irradiation, large bubbles with extremely small number density are formed during pre-irradiation, and the small bubbles are newly formed with large number density during following irradiation.

The difference among bubble formation and growth depending on the mode of irradiation is considered to be mainly due to a difference in the production rate of point defects produced by H_2^+ and He^+ ion irradiations and the different mobility of hydrogen and helium atoms injected by irradiation in aluminum.

References

[1] ISHINO S., KAWANISHI M., FUKUYA K. and MUROGA T., *IEEE. Trans. Nucls. Sci.* **NS-30** (1983) 1255.
[2] TAKEYAMA T., OHNUKI H. and TAKAHASHI H., *J. Nucl. Mater.* **133-134** (1985) 571.
[3] HOJOU K., FURUNO S., IZUI K. and TSUKAMOTO T., *J. Nucl. Mater.* **155-157** (1988) 298.
[4] FURUNO S., HOJOU K., IZUI K., KAMIGAKI N. and KINO T., *J. Nucl. Mater.* **155-157** (1988) 1149.
[5] FURUNO S., HOJOU K., OTSU H., IZUI K., KAMIGAKI N. and KINO T., *J. Nucl. Mater.* **179-181** (1991) 1011.
[6] FURUNO S., HOJOU K., OTSU H., IZUI K., SASAKI T.A., TSUKAMOTO T. and HATA T., *J. Electron Microsc.* **41** (1992) 273.
[7] FURUNO S., HOJOU K., IZUI K., KAMIGAKI N., ONO K. and KINO T., *J. Nucl. Mater.* **191-194** (1992) 1219.
[8] KINO T., HASHIMOTO E., KAMIGAKI N., KISO K. and MATSUSHITA R., *Trans. Jpn. Inst. Met.* **18** (1977) 305.
[9] ELLS C.L. and EVANS W., AECL-1286, Chalk River, Ontario, May (1961).